Tunable few-electron double quantum dots with integrated charge read-out

J.M. Elzerman[a,*], R. Hanson[a], J.S. Greidanus[a], L.H. Willems van Beveren[a], S. De Franceschi[a], L.M.K. Vandersypen[a], S. Tarucha[b,c], L.P. Kouwenhoven[a]

[a] Kavli Institute of NanoScience Delft and ERATO Mesoscopic Correlation Project, Delft University of Technology, P.O. Box 5046, 2600 GA Delft, Netherlands
[b] NTT Basic Research Laboratories, Atsugi-shi, Kanagawa 243-0129, Japan
[c] ERATO Mesoscopic Correlation Project, University of Tokyo, Bunkyo-ku, Tokyo 113-0033, Japan

Available online 3 August 2004

Abstract

We report on the realization of few-electron double quantum dots defined in a two-dimensional electron gas by means of surface gates on top of a GaAs/AlGaAs heterostructure. Two quantum point contacts (QPCs) are placed in the vicinity of the double quantum dot and serve as charge detectors. These enable determination of the number of conduction electrons on each dot. This number can be reduced to zero, while still allowing transport measurements through the double dot. The coupling between the two dots can be controlled even in the few-electron regime. Microwave radiation is used to pump an electron from one dot to the other by absorption of a single photon. The experiments demonstrate that this quantum dot circuit can serve as a good starting point for a scalable spin-qubit system.
© 2004 Elsevier B.V. All rights reserved.

The experimental development of a quantum computer is at present in the stage of realizing few-qubit circuits. In the solid state, particular success has been achieved with superconducting devices in which macroscopic quantum states are used to define two-level qubit states (see Ref. [1] and references therein). The opposite alternative would be the use of two-level systems defined by microscopic variables, as realized for instance by single electrons confined in semiconductor quantum dots [2]. For the control of one-electron quantum states by electrical voltages, the challenge at the moment is to realize an appropriate quantum dot circuit containing just a single conduction electron.

Few-electron quantum dots have been realized in self-assembled structures [3] and also in small vertical pillars, defined by etching [4]. The disadvantage of these types of quantum dots is that they are hard to integrate into circuits with a controllable coupling between the elements, although integration of vertical quantum dot

*Corresponding author.

structures is currently being pursued [5]. An alternative candidate is a system of lateral quantum dots defined in a 2-dimensional electron gas (2DEG) by surface gates on top of a semiconductor heterostructure [2]. Here, integration of multiple dots is straightforward by simply increasing the number of gate electrodes. In addition, the coupling between the dots can be controlled, since it is set by gate voltages. The challenge is to reduce the number of electrons to one per quantum dot. This has long been impossible, since reducing the electron number decreases, at the same time, the tunnel coupling, resulting in a current too small to be measured [6].

We demonstrate double quantum dot devices containing a voltage-controllable number of electrons down to a single electron. We have integrated these devices with charge detectors that can read-out the charge state of the double quantum dot with a sensitivity better than a single electron charge. The importance of the present circuits is that they can serve as fully tunable two-qubit quantum systems, following the proposal by Loss and DiVincenzo [7], which describes an optimal combination of the single-electron charge degree of freedom (for manipulation with electrical voltages) and the spin degree of freedom (to obtain a long coherence time).

We study two nominally identical devices, both as shown in Fig. 1a. They are made from a GaAs/AlGaAs heterostructure that contains a 2DEG 90 nm below the surface with an electron density, $n_s = 2.9 \times 10^{11}$ cm^{-2}. Both devices consist of a double quantum dot and two quantum point contacts (QPCs). The layout is an extension of previously reported single quantum dot devices [6]. The double quantum dot is defined by applying negative voltages to the 6 gates in the middle of the figure. Gate T in combination with the left (right) gate, $L(R)$, defines the tunnel barrier from the left (right) dot to drain 1 (source 2). Gate T in combination with the middle, bottom gate, M, defines the tunnel barrier between the two dots. The narrow "plunger" gate, P_L (P_R), on the left (right) is used to change the electrostatic potential of the left (right) dot. The plunger gates can be connected to a coaxial cable, so that we can apply high-frequency signals. In the present experiments,

we do not apply dc voltages to P_L. In order to control the number of electrons on the double dot, we use gate L for the left dot and P_R or R for the right dot. All measurements are performed at a temperature of 10 mK.

We first study sample 1. We characterize the individual dots using standard Coulomb blockade experiments [2], and find that the energy cost for adding a second electron to a one-electron dot is 3.7 meV. The excitation energy (i.e. the difference between the first excited state and the ground state) is 1.8 meV at zero magnetic field. For a two-electron dot, the energy difference between the singlet ground state and the triplet excited state is 1.0 meV at zero magnetic field. Increasing the field (perpendicular to the 2DEG) leads to a transition from a singlet to a triplet ground state at about 1.7 T.

In addition to current flowing through the quantum dot, we can measure the charge on the dot using one of the QPCs [8,9]. We define only the left dot (by grounding gates R and P_R), and use the left QPC as a charge detector. The QPC is formed by applying negative voltages to Q-L and L. This creates a narrow constriction in the 2DEG, with a conductance, G, that is quantized when sweeping the gate voltage V_{Q-L}. The plateau at $G = 2e^2/h$ and the transition to complete pinch-off (i.e. $G = 0$) are shown in Fig. 1b. At the steepest point, where $G \approx e^2/h$, the QPC-conductance has a maximum sensitivity to changes in the electrostatic environment, including changes in the charge of the nearby quantum dot. As seen in Fig. 1b, the QPC-current, I_{QPC}, decreases when we make the left-dot gate voltage, V_M, more negative. Periodically, this changing gate voltage pushes an electron out of the left dot. The associated sudden change in charge increases the electrostatic potential in the QPC, resulting in a step-like structure in I_{QPC} (see expansion in Fig. 1b, where the linear background is subtracted). So, even without passing current through the dot, I_{QPC} provides information about the charge on the dot. To enhance the charge sensitivity, we apply a small modulation (0.3 mV at 17.7 Hz) to V_M and use lock-in detection to measure dI_{QPC}/dV_M [9]. Fig. 1c shows the resulting dips, as well as the corresponding Coulomb peaks measured in the
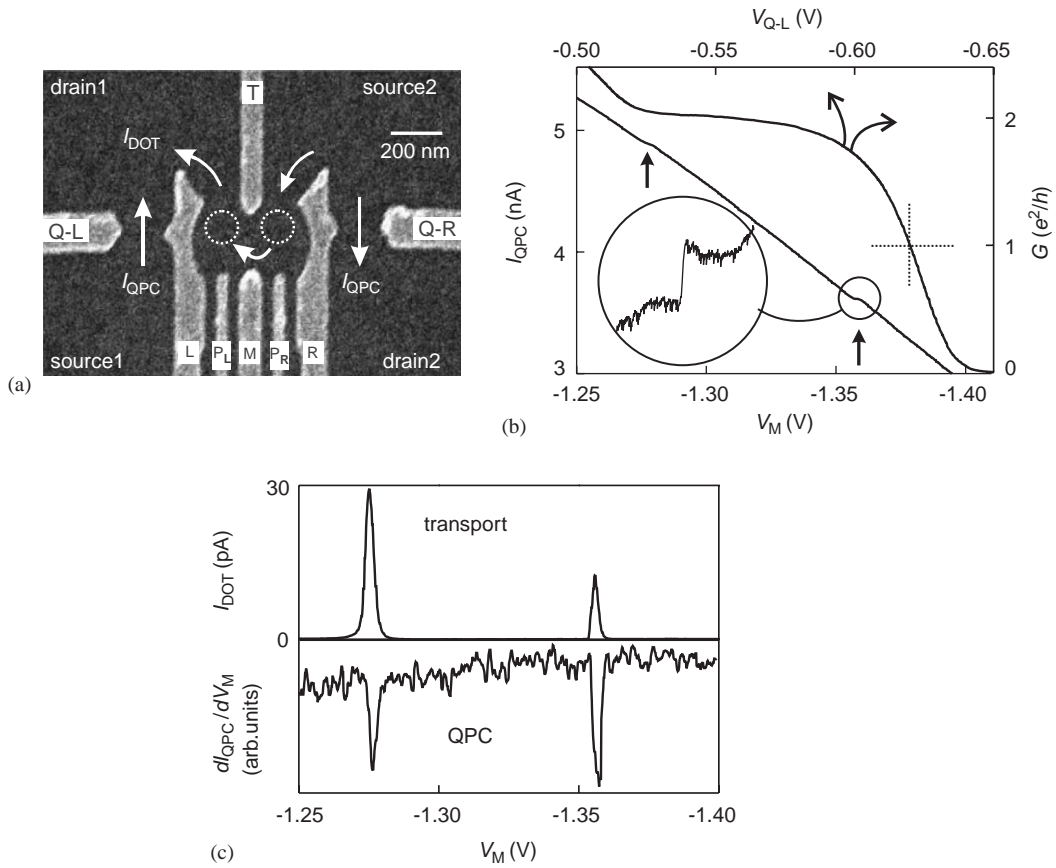
Fig. 1. (a) Scanning electron micrograph of the metallic surface gates. White dotted circles indicate the two quantum dots. White arrows show the possible current paths. A bias voltage, V_{DOT}, can be applied between source 2 and drain 1, leading to current through the dots, I_{DOT}. A bias voltage, V_{SD1} (V_{SD2}), between source 1 (source 2) and drain 1 (drain 2), yields a current, I_{QPC}, through the left (right) QPC. (b) QPC as a charge detector of the left single dot. Upper curve with upper and right axis: conductance, G, of the left QPC versus the gate voltage, V_{Q-L}, showing the last quantized plateau and the transition to complete pinch-off. The dashed line indicates the point of highest charge sensitivity. Lower curve with lower and left axis: current through the left QPC, I_{QPC}, versus left-dot gate voltage, V_M. ($V_{SD1} = 250\ \mu V$, $V_{DOT} = 0$, $V_{SD2} = 0$). The steps, indicated by the arrows, correspond to a change in the electron number of the left dot. Encircled inset: the last step (50 pA high), with the linear background subtracted. (c) Upper part: Coulomb peaks measured in transport current through the left dot. Shown is I_{DOT} versus V_M with $V_{DOT} = 100\ \mu V$. Lower part: changes in the number of electrons on the left dot, measured with the left QPC. Shown is dI_{QPC}/dV_M versus V_M ($V_{SD1} = 250\ \mu V$, $V_{DOT} = 0$).

current through the dot. The coincidence of the two signals demonstrates that the QPC indeed functions as a charge detector. From the height of the step in Fig. 1b (50 pA, typically 1–2% of the total current), compared to the noise (5 pA for a measurement-time of 100 ms), we can estimate the sensitivity of the charge detector to be about $0.1e$, with e being the single electron charge. The important advantage of QPC charge detection is that it provides a signal even when the tunnel barriers of the dot are so opaque that I_{DOT} is too small to measure [8,9]. This allows us to study quantum dots even while they are virtually isolated from the leads.

Next, we study the charge configuration of the double dot, using the QPC on the right as a charge detector. We measure dI_{QPC}/dV_L versus V_L, and repeat this for many values of V_{PR}. The resulting two-dimensional plot is shown in Fig. 2a. Dark lines signify a negative dip in dI_{QPC}/dV_L,
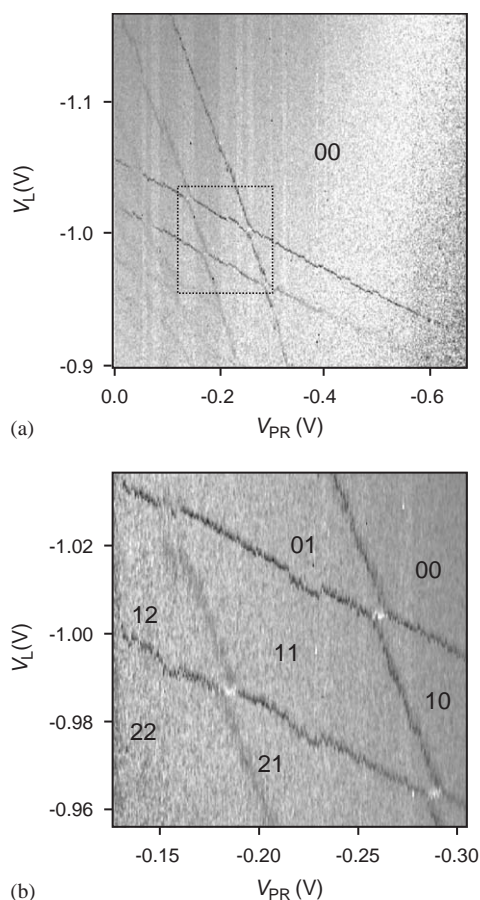
Fig. 2. (a) Charge stability diagram ("honeycomb") of the double quantum dot, measured with $Q - R$. A modulation (0.3 mV at 17.77 Hz) is applied to gate L, and dI_{QPC}/dV_L is measured with a lock-in amplifier and plotted in grayscale versus V_L and V_{PR}. The bias voltages are: $V_{SD2} = 100\ \mu V$ and $V_{DOT} = V_{SD1} = 0$. The label "00" indicates the region where the double dot is completely empty. (b) Zoom-in of (a), showing the honeycomb pattern for the first few electrons in the double dot. The black labels indicate the number of electrons in the left and right dot.

corresponding to a change in the total number of electrons on the double dot. Together, these lines form the well-known "honeycomb diagram" [10,11]. The almost-horizontal lines correspond to a change in the electron number in the left dot, whereas almost-vertical lines indicate a change of one electron in the right dot. In the upper left region, the "horizontal" lines are not present, even though the QPC can still detect changes in the

charge, as demonstrated by the presence of the "vertical" lines. We conclude that in this region, the left dot contains zero electrons. Similarly, a disappearance of the "vertical" lines occurs in the lower right region, showing that here the right dot is empty. In the upper right region, the absence of lines shows that here the double dot is completely empty.

We are now able to count the absolute number of electrons. Fig. 2b shows a zoom-in of the few-electron region. Starting from the "00" region, we can label all regions in the honeycomb diagram, e.g. the label "21" means two electrons in the left dot and one in the right. Besides the dark lines, also short white lines are visible, signifying a positive peak in dI_{QPC}/dV_L. These white lines correspond to a charge transition between the dots, while the total electron number remains the same. (The positive sign of dI_{QPC}/dV_L can be understood if we note that crossing the white lines by making V_L a little more positive means moving an electron from the right to the left dot, which increases I_{QPC}. Therefore, the differential quantity dI_{QPC}/dV_L displays a positive peak.) The QPC is thus sufficiently sensitive to detect *inter-dot* transitions.

In measurements of transport through lateral double quantum dots, the few-electron regime has never been reached [11]. The problem is that the gates, used to deplete the dots, also strongly influence the tunnel barriers. Reducing the electron number would always lead to the Coulomb peaks becoming unmeasurably small, but not necessarily due to an empty double dot. The QPC detectors now permit us to compare charge and transport measurements. Fig. 3a shows I_{DOT} versus V_L and V_{PR}, with the dotted lines extracted from the measured charge lines in Fig. 2b. In the bottom left region, the gates are not very negative, hence the tunnel barriers are quite open. Here, the resonant current at the charge transition points is quite high (~ 100 pA, dark gray), and also lines due to cotunneling are visible [11]. Towards the top right corner, the gate voltages become more negative, thereby closing off the barriers and reducing the current peaks (lighter gray). The last Coulomb peaks (in the dashed square, and in Fig. 3b) are faintly visible (~ 1 pA). Apart from a
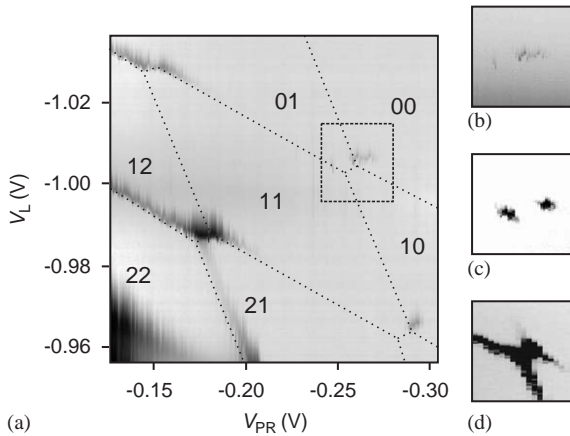
Fig. 3. (a) Transport through the double dot in the same region as Fig. 2b. Plotted on the logarithmic grayscale is I_{DOT} versus V_L and V_{PR}, with $V_{DOT} = 100$ μV and $V_{SD1} = V_{SD2} = 0$. The dotted lines are extracted from Fig. 2b. In the light regions, current is zero due to Coulomb blockade. Dark gray indicates current, with the darkest regions (in the bottom left corner) corresponding to ~ 100 pA. Inside the dashed square, the last Coulomb peaks are visible (~ 1 pA). (A smoothly varying background current due to a small leakage from a gate to the 2DEG has been subtracted from all traces.) (b) Close-up of the region inside the dashed square in (a), showing the last two triple points before the double dot is completely empty. The current at these triple points is very small (~ 1 pA) since the tunnel barriers are very opaque. (c) Last two triple points for different values of the voltage applied to the gates defining the tunnel barriers. For these settings, the two triple points are clearly separated. The current at the triple points is about 5 pA. The cotunneling current is not visible. (d) Last two triple points, but now with the gate voltages such that the barriers defining the double dot are very transparent. The current at the triple points is about 70 pA, and the cotunneling current is clearly visible.

slight shift, the dotted lines nicely correspond to the regions where a transport current is visible. We are thus able to measure transport through a one-electron double quantum dot.

Even in the few-electron regime, the double dot remains fully tunable. By changing the voltage applied to gate T, we can make the tunnel barriers that define the double dot more transparent, leading to a larger current through the device. We use this procedure to increase the current at the last two triple points. For the gate voltages used in Fig. 3b, the resonant current is very small (~ 1 pA), and the triple points are faintly visible. By making V_T less negative, the resonant current

becomes about 5 pA (Fig. 3c). The cotunneling current is not visible, and the two triple points are clearly separated. By changing V_T even more, the current at the last triple points can be increased to ~ 70 pA (Fig. 3d). For these settings, the triple points have turned into lines, due to the increased cotunneling current. This sequence demonstrates that we can tune the double dot from being nearly isolated to being very transparent.

We can also control the inter-dot coupling, by changing the voltage applied to gate M. This is demonstrated with a QPC charge measurement using sample 2. We apply a square wave modulation of 3 mV at 235 Hz to the rightmost plunger gate, P_R, and dI_{QPC}/dV_{PR} is measured using a lock-in amplifier. Fig. 4a shows the familiar honeycomb diagram in the few-electron regime. All lines indicating charge transitions are very straight, implying that for the gate settings used, the tunnel-coupling between the two dots is negligible, compared to the capacitive coupling. This is the so-called "weak-coupling" regime. (We note that the double dot, as a whole, is still quite well-coupled to the leads, so that the total number of electrons can change, as demonstrated by the regular shape of the honeycomb pattern [12].) By making V_M less negative, the tunnel barrier between the two dots is made more transparent, and the "intermediate-coupling" regime is reached (Fig. 4b). Most lines are still straight, except in the bottom left corner, where they are slightly bent. This signifies that here the inter-dot tunnel-coupling is comparable to the capacitive coupling. If we make V_M even less negative, we reach the strong-coupling regime (Fig. 4c). In this case, all lines are very curved, implying that the tunnel-coupling is dominating over the capacitive coupling. Thus the double dot behaves more like a single dot in this regime.

The use of gated quantum dots for quantum state manipulation in time requires the ability to modify the potential at high frequencies. We investigate the high-frequency behavior in the region around the last Coulomb peaks (Fig. 5a) in sample 1, with a 50 GHz microwave-signal applied to gate P_L. At the dotted line, the 01 and 10 charge states are degenerate in energy, so one electron can tunnel back and forth between the
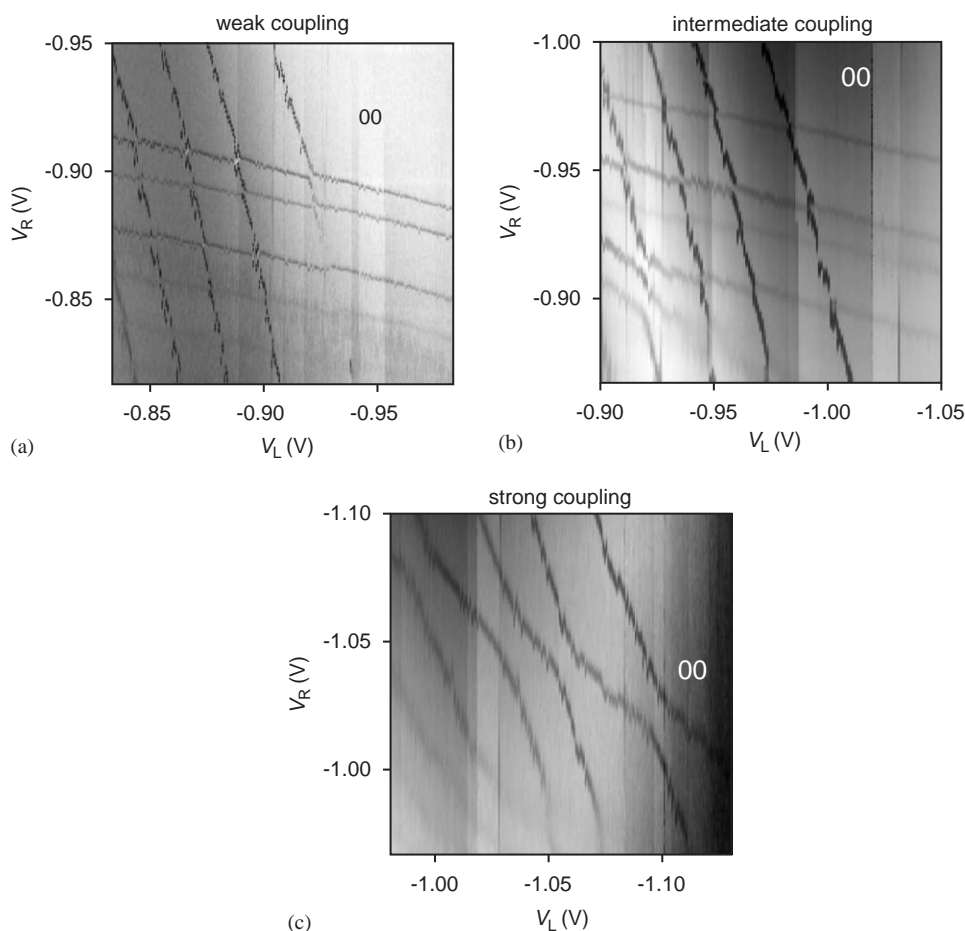
Fig. 4. Controlling the inter-dot coupling with V_M. The charge stability diagrams of the double quantum dot are measured using Q-L in sample 2. A modulation (3 mV at 235 Hz) is applied to gate PR, and dI_{QPC}/dV_{PR} is measured with a lock-in amplifier and plotted in grayscale versus V_L and V_R. A magnetic field of 6 T is applied in the plane of the 2DEG. (a) Weak-coupling regime. V_M is such that all dark lines, indicating charge transitions, are straight. The tunnel-coupling between the two dots is negligible compared to the capacitive coupling. (b) Intermediate-coupling regime. V_M is 0.07 V less negative than in (a), such that lines in the bottom left corner are bent. This signifies that here the inter-dot tunnel-coupling is comparable to the capacitive coupling. (c) Strong-coupling regime. V_M is 0.1 V less negative than in (b), such that all lines are very curved. This implies that the tunnel-coupling is dominating over the capacitive coupling and the double dot behaves as a single dot.

two dots. Away from this line, there is an energy difference and only one charge state is stable. However, if the energy difference matches the photon energy, the transition to the other dot is possible by absorption of a single photon. Such photon-assisted tunneling events give rise to the two lines indicated by the arrows. At the lower (higher) line, electrons are pumped from the left (right) dot to the other side, giving rise to a negative (positive) photon-assisted current. We

find that the distance between the two photon-assisted tunneling lines, ΔV_L, scales linearly with frequency (Fig. 5b), as expected [11].

The realization of a controllable few-electron quantum dot circuit represents a significant step towards controlling the coherent properties of single electron spins in quantum dots [7,13]. Integration with the QPCs permits charge read-out of closed quantum dots. We note that charge read-out only affects the spin state indirectly, via
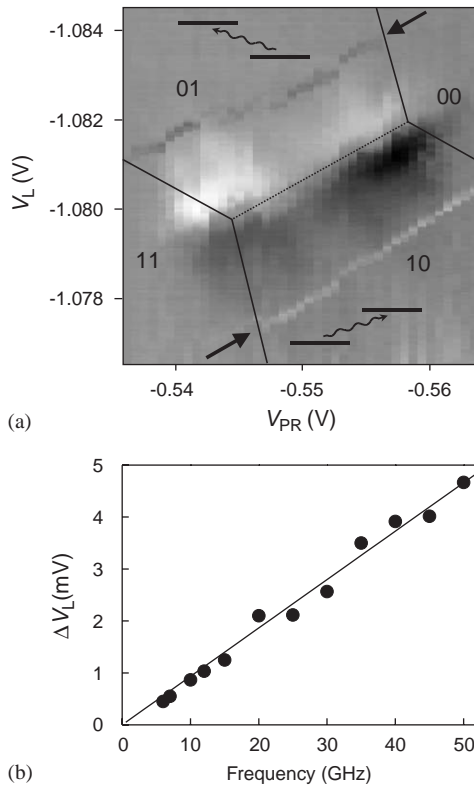
(a)

(b)

Fig. 5. (a) Photon-assisted transport through the double dot, with zero bias voltage, i.e. $V_{DOT} = V_{SD1} = V_{SD2} = 0$. A microwave signal of 50 GHz is applied to P_L, in sample 1. The microwaves pump a current, I_{DOT}, by absorption of photons. This photon-assisted current shows up as two lines, indicated by the two arrows. The white line (bottom) corresponds to pumping from the left to the right reservoir, the dark line (top) corresponds to pumping in the reverse direction. In the middle, around the dotted line, a finite current is induced by an unwanted voltage drop over the dot, due to asymmetric coupling of the ac-signal to the two leads [11]. (b) Separation between the two photon-assisted tunneling lines versus microwave frequency. The dependence is linear down to the lowest frequency of about 6 GHz.

the spin-orbit interaction. The back-action on the spin should therefore be small (until spin-to-charge conversion is initiated), and can be further suppressed by switching on the charge detector only during the read-out stage. Present experiments focus on increasing the speed of the charge measurement such that single-shot read-out of a single electron spin could be accomplished [13,14].

References

[1] D. Vion, A. Aassime, A. Cottet, P. Joyez, H. Pothier, C. Urbina, D. Estève, M.H. Devoret, Science 296 (2002) 886.
[2] L.P. Kouwenhoven, C.M. Marcus, P.L. McEuen, S. Tarucha, R.M. Westervelt, N.S. Wingreen, in: L.L. Sohn, L.P. Kouwenhoven, G. Schön (Eds.), Mesoscopic Electron Transport, NATO Advanced Study Institutes, Ser. E, Vol. 345, Kluwer, Dordrecht, Boston, 1997, pp. 105–214.
[3] P.M. Petroff, A. Lorke, A. Imamoglu, Phys. Today 46 (May 2001).
[4] L.P. Kouwenhoven, D.G. Austing, S. Tarucha, Rep. Prog. Phys. 64 (6) (2001) 701.
[5] K. Ono, D.G. Austing, Y. Tokura, S. Tarucha, Science 297 (2002) 1313.
[6] M. Ciorga, A.S. Sachrajda, P. Hawrylak, C. Gould, P. Zawadzki, S. Jullian, Y. Feng, Z. Wasilewski, Phys. Rev. B 61 (2000) R16315.
[7] D. Loss, D.P. DiVincenzo, Phys. Rev. A 57 (1998) 120.
[8] M. Field, C.G. Smith, M. Pepper, D.A. Ritchie, J.E.F. Frost, G.A.C. Jones, D.G. Hasko, Phys. Rev. Lett. 70 (1993) 1311.
[9] D. Sprinzak, Y. Ji, M. Heiblum, D. Mahalu, H. Shtrikman, Phys. Rev. Lett. 88 (2002) 176805.
[10] H. Pothier, P. Lafarge, C. Urbina, D. Estève, M.H. Devoret, Europhys. Lett. 17 (1992) 249.
[11] W.G. van der Wiel, S. De Franceschi, J.M. Elzerman, T. Fujisawa, S. Tarucha, L.P. Kouwenhoven, Rev. Mod. Phys. 75 (2003) 1 see also cond-mat/0205350v2.
[12] A.W. Rushforth, C.G. Smith, M.D. Godfrey, H.E. Beere, D.A. Ritchie, M. Pepper, Phys. Rev. B 69 (2004) 113309.
[13] L.M.K. Vandersypen, R. Hanson, L.H. Willems van Beveren, J.M. Elzerman, J.S. Greidanus, S. De Franceschi, L.P. Kouwenhoven, in: A.J. Legget, B. Ruggiero, P. Silvestrini (Eds.), Quantum Computing and Quantum Bits in Mesoscopic Systems, Kluwer Academic/Plenum Publishers, New York, 2003. see also quant-ph/0207059, 2002.
[14] A. Aassime, G. Johansson, G. Wendin, R.J. Schoelkopf, P. Delsing, Phys. Rev. Lett. 86 (2001) 3376.